Theoretical Study of a New Building Block for Organic Conductors: Tetrathiapentalene and Its Radical Cation

Carlo Adamo,*,† Roger Arnaud,‡ Giovanni Scalmani,† Harald Müller,§ Fouad Sahli,§ and Vincenzo Barone†

Dipartimento di Chimica, Università "Federico II", via Mezzocannone 4, I-80134 Napoli, Italy, Laboratoire d'Études Dynamiques et Structurales de la Sélectivité (LEDSS), UMR CNRS 5616, Université Joseph Fourier, 301 Avenue de la Chimie, BP 53X, F-38041 Grenoble Cedex 09, France, and European Synchrotron Radiation Facility (ESRF), BP 200 F-38043 Grenoble Cedex 9, France

Received: March 17, 1999; In Final Form: June 2, 1999

The molecular properties of tetrathiapentalene (TTP), a new and promising building block for conducting organic polymers, and of its radical cation have been studied by a hybrid Hartree−Fock/Kohn−Sham method. Parallel computations have been performed for tetrathiafulvalene (TTF), a well-known component of many organic conductors, with the aim of understanding the potentialities of TTP. Our results show that geometrical parameters and vibrational frequencies of radical cations are similar for TTF and TTP, thus suggesting that comparable bulk properties can be expected for both molecules. At the same time, the larger spin delocalization on terminal carbon atoms of TTP^+ explains its greater reactivity.

1. Introduction

A contemporary challenge in molecular chemistry is to design, with a wise choice of the constituent molecules, new materials that couple properties not normally associated with a single constituent. Examples include hybrid molecular materials combining a magnetic component, typically an inorganic network containing transition metal ions, with an organic conducting component, usually a π-electron donor or acceptor.[1] In this context the two main issues are the creation of molecule-based materials with a coexistence of properties (e.g. ferromagnetism and superconductivity) and the preparation of molecular hybrids exhibiting a coupling between localized d-electrons and conduction π-electrons.[2] Successful results have been obtained by employing cation radical salts formed by organic donor molecules of the tetrathiafulvalene type (TTF, see Figure 1) and its derivatives with magnetic counterions.[3,4]

TTF and its derivatives act as π-electron donors and represent reversible two-step redox systems capable of forming stable monoradical cations[5−8] and dications,[9] both in solution and in the solid state. Due to this peculiar behavior, tetrathiafulvalenes are becoming essential building blocks in the rapidly evolving field of molecular conductors and superconductors.[10]

One key feature ruling the conducting properties of such species is their conformation. In fact all the donor molecules for organic superconductors are characterized by distorted boat conformations in the neutral forms, but by planar conformations for the corresponding radical cations. This peculiar conformational behavior may be responsible for the properties of these compounds, since conduction leads to a coupling between charge transfer and the boat deformation phonon mode.[11]

A series of disubstituted derivatives has been synthesized very recently with the aim of preparing vinyloguous dimeric, oligomeric, and polymeric tetrathiafulvalenes starting from tetrathiapentalene precursors (TTP; see Figure 2),[12,13] even if TTP itself has not yet been characterized. The successful realization of this synthetic approach is essentially based on the transformation tetrathiapentalene → tetrathiafulvalene via radical−radical coupling of the intermediate TTP radical cation.[13] The sequence takes advantage of the apparent instability and thus high reactivity of TTP radicals, a behavior which contrasts sharply with what is known for the corresponding TTF isomer.[12] A full characterization of TTP monomer molecule and its radical cation is a mandatory prerequisite for better understanding of the physicochemical properties of TTP derivatives. In particular, the spin distribution, as well as the related magnetic behavior, in the radical cations of TTP is of interest for understanding the properties of the corresponding organic metals. Unfortunately, the apparent instability of TTP precludes a detailed experimental analysis.

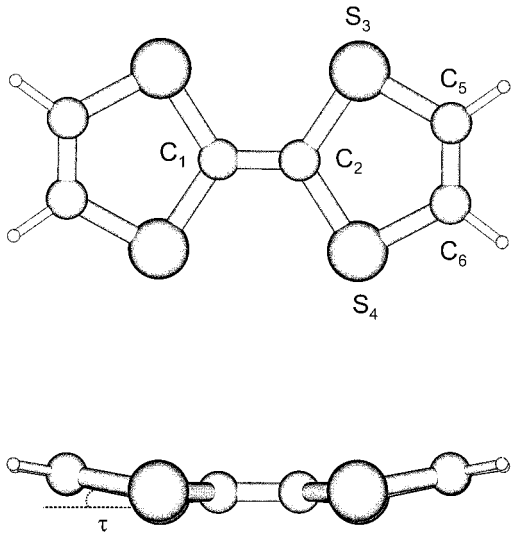

Figure 1. Structure and atom labeling for tetrathiafulvalene.

In such circumstances, quantum mechanical approaches can offer a valuable support to experiment. Of course, they must

* Corresponding author. E-mail: adamo@chemna.dichi.unina.it.
† Università "Federico II".
‡ Université Joseph Fourier.
§ ESRF.

10.1021/jp990940+ CCC: $18.00
Published on Web 07/27/1999

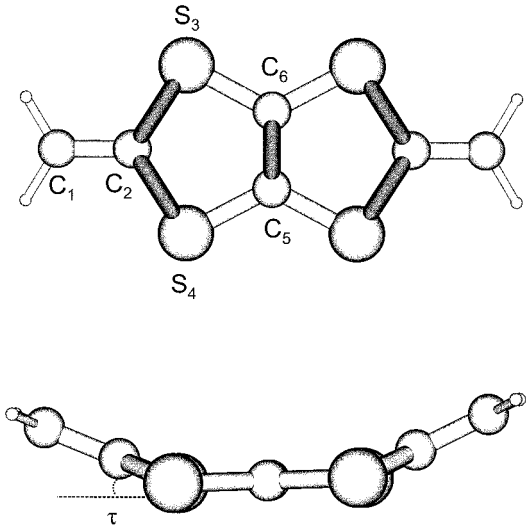

Figure 2. Structure and atom labeling for tetrathiapentalene.

TABLE 1: Main Geometrical Parameters (Bond Lengths, Å; Valence and Dihedral Angles, deg) for TTF, TTP, and Their Radical Cations[a]

	TTF				TTP	
	molecule	expt[b]	expt[c]	radical	molecule	radical
C_1C_2	1.346	1.358	1.349	1.395	1.339	1.337
C_2C_3	1.787	1.767	1.748	1.647	1.795	1.783
S_3C_5	1.761	1.753	1.729	1.627	1.764	1.730
C_5C_6	1.333	1.348	1.314	1.423	1.337	1.385
$C_1C_2S_3$	123.1		1.227	122.4	123.0	122.8
$C_2S_3C_5$	95.0	94.5	94.5	97.8	94.7	95.1
$S_3C_5C_6$	118.1		118.0	114.7	118.3	117.8
$S_3C_2S_4$					114.0	114.4
τ	9.9	166.5		0.0	8.5	0.0

[a] All of the parameters have been computed at the B1LYP/6-311G(d) level. Atom labeling is reported in Figures 1 and 2. [b] Electron diffraction data. [c] X-ray data.[44]

provide reliable structural and magnetic properties, in particular for large systems, like those of interest in the present work.

In this connection, several studies have shown that methods rooted in the density functional (DF) theory give remarkably accurate results for electronic and magnetic properties of organic radicals.[14−22] In particular, hybrid Hartree−Fock/Kohn−Sham (HF/KS) approaches seem to be the most effective computational tools.[23−26] Following this direction, we have recently introduced a "parameter free" hybrid approach,[27,28] which provides even better estimates of magnetic properties.[27,29]

Here we apply this computational protocol to the analysis of the structure and spectroscopic (IR and EPR) properties of TTP and its radical cation. The goal of this study is to understand, through a detailed comparison with the well-known TTF molecule, if TTP can become a new powerful molecular brick in the field of organic metals.

Due to their exciting solid-state properties, a great deal of information on the electronic structure of tetrathiafulvalenes is available from quantum mechanical calculations (see for instance refs 30−33). In contrast very little is known about TTP, even if its electronic structure is iso-π-electronic to TTF, thus suggesting similar conducting properties.

Our investigations will cover not only the two neutral molecules but also the corresponding radical cations (hereafter TTF^+ and TTP^+), which are fundamental components of organic conductors. It must be pointed out also that, to the best of our knowledge, this is the first time that a detailed theoretical analysis has been carried out on the spectroscopic properties of the TTF^+ radical cation.

2. Computational Details

Density functional calculations were carried out within the unrestricted Kohn−Sham (UKS) formalism, as implemented in the Gaussian 98 code[34] and using the so-called B1LYP hybrid functional[27] obtained combining HF and Becke[36] exchange terms in a predefinite amount (1:4) together with the Lee−Yang−Parr correlation functional.[37]

The 6-311G(d,p) basis set of Pople and co-workers[38] has been used for all geometry optimizations, since previous experience showed that a polarized valence triple-ζ basis set provides essentially converged structural parameters by DF methods.[39,40] Improved magnetic properties were obtained by the EPR-II basis set, which was specifically optimized for this purpose.[16,41]

Isotropic hyperfine coupling constants (hcc's) a_N are related to the spin densities at the corresponding nuclei by[42]

$$a_N = \frac{8\pi}{3\hbar} g_e \beta_e g_N \beta_N \sum_{\mu,\nu} P^{\alpha-\beta}_{\mu,\nu} \langle \varphi_\mu | \delta(r_{kN}) | \varphi_\nu \rangle \qquad (1)$$

where β_e, β_N are the electron and nuclear magnetons, respectively, g_e, g_N are the corresponding magnetogyric ratios, $\hbar$ is the Planck constant, $\delta(\mathbf{r})$ is a Dirac delta operator, and $P^{\alpha-\beta}$ is the difference between the density matrices for electrons with α and β spin. In the present work, all the values are given in Gauss (1 G = 0.1 mT), assuming that the free electron g value is appropriate also for the radicals. To convert data to megahertz, one has to multiply them by 2.8025.

All drawings, including spin density representations, have been obtained by the Molden package.[43]

3. Results and Discussion

As mentioned above there are no experimental data concerning the TTP molecule or the TTP^+ radical, whereas TTF and TTF^+ have been characterized by X-ray and electron diffraction structures,[44−46] infrared,[47,48] and electron paramagnetic resonance (EPR)[5−8] spectra. A detailed comparison between these data and our quantum mechanical results will underline the limits of our computational approach.

3.1. Geometrical Features. In Table 1 are reported the most relevant geometrical parameters for TTP, TTF, and their radical cations, while atom labeling is shown in Figures 1 and 2.

The most striking feature of TTP and TTF molecules is their nonplanarity. As mentioned in the Introduction, one of the characteristics of TTF is the floppy inversion motion between a C_{2v} conformation (boat arrangement) and a D_{2h} planar structure. In contrast, the radical cation is planar.[32] This behavior is common for organic superconductors which exhibit distorted boat conformations in their neutral forms, but planar conformations in the corresponding cationic states X^+.[32]

Previous MP2 computations suggest a floppy inversion motion in TTF, governed by a bare potential energy barrier of 0.55 kcal/mol.[32] Furthermore, B3LYP computations, carried out with a medium-size basis set, predict that the planar structure becomes the most stable when zero point effects (ZPE) are taken into account.[33]

Our computations are in agreement with this last result. In fact, the boat conformation of the TTF molecule is an energy minimum at the B1LYP/6-311G(d,p) level, with an out of plane angle of 9.9° (τ; see Figure 1) and the planar structure is a first-order saddle point (SP), 0.05 kcal/mol higher in energy, characterized by one imaginary frequency of $21i$ cm^{-1}. Similar behavior has been found for TTP. In fact, the minimum energy

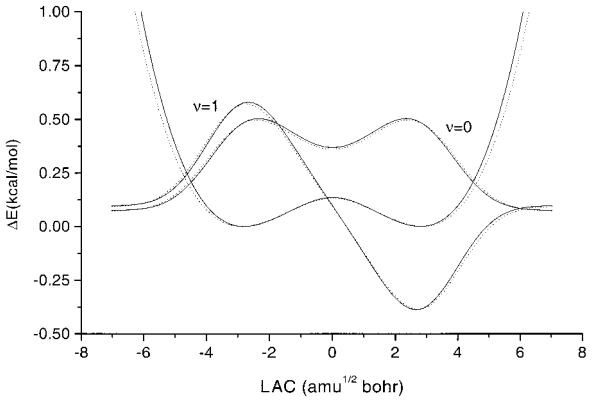

Figure 3. Potential energy and vibrational wave functions (normalized to 10) for the inversion motion of TTF in vacuo (full line) and in aqueous solution (broken line).

conformation of TTP has C_{2v} symmetry and can be described as a boat arrangement with $\tau = 8.5°$ (see Figure 1). The corresponding planar conformation is a SP 0.10 kcal/mol higher in energy and with one imaginary frequency of $35i$ cm^{-1}.

A better description of the situation is obtained by treating the inversion motion by the so-called distinguished coordinate (DC) approach,[41] in which all the other geometrical parameters are optimized at selected values of the out of plane angle τ (see Figure 1). The distance between successive points in mass-weighted Cartesian coordinates defines the so-called Large Amplitude Coordinate (LAC). Using the corresponding potential energy curves, vibrational wave functions have been computed by the numerical procedures implemented in the DiNa program.[49,50] From the results it is quite evident that the first vibrational level is always very close to the potential energy barrier, so that both TTF and TTP are best described as quasi-planar molecules with large amplitude inversion modes. Modulation of the inversion motion by solvent has been next investigated by the polarizable continuum model (PCM) recently implemented by one of us in the Gaussian package.[51,52] Although some small effects can be evidenced, general trends remain essentially unmodified. For purposes of illustration the potential energy and vibrational wave functions for the inversion of TTF are shown in Figure 3, both for the isolated system and for its aqueous solution.

Ionizing the molecules leads to a strong preference for planarity that overcomes any strain effect, inducing a planar conformation for radicals. This is, of course, the direct effect of the increased conjugation in the thiole rings issuing from ionization.

The preference for a planar structure in the radicals is quite evident if the remaining geometrical parameters are analyzed. For instance the C1C2 bond length increases significantly in going from TTF to TTF$^+$ (1.346 vs 1.395 Å), and the same occurs for the C5C6 distance (from 1.333 to 1.423 Å). So both bonds lose some of their double bond character. In contrast the CS bonds (C2S3 and C5S3) are shortened (by 0.14 Å), becoming close to typical double bonds. As a consequence the molecular structure of TTF$^+$ is best described in terms of two separate thiole rings joined by a single CC bond.

The same trends are observed for TTP$^+$, although all the geometry modifications are smaller. So in the radical the C2S3 and S3C5 bonds are shortened by 0.03 and 0.01 Å, respectively, with respect to the parent neutral system, while the C5C6 bond is slightly lengthened (by 0.05 Å), and the C1C2 bond remains unchanged.

These variations in going from the neutral molecules to the radical cations are well-reflected in the vibrational spectra, whose computed wavenumbers are reported in Table 2, together with an approximate assignment.

To put in better evidence the difference between molecules and radicals, the assignment and symmetry labels refer to the C_{2v} point group, even if both radicals have D_{2h} symmetry. In the same table are reported the observed wavenumbers for TTF.[48] Since our DF results do not differ significantly from those already reported,[33] we do not discuss in detail the vibrational assignment or the comparison with experimental values, focusing rather our attention on the difference between neutral and cationic species.

A detailed analysis of the data reported in Table 2 shows that four sets of vibrations are affected by ionization, namely, the CC and CS stretchings, the CC bending, and the CH out of plane motions. In particular, in going from TTF to TTF$^+$ the stretching frequencies associated with the central C1C2 bond decrease by 88 and 144 cm^{-1} for the $2a_1$ and $3a_1$ modes, respectively. Less evident is the variation of the mode associated with the C5C6 bond ($1b_2$), whose frequency is reduced by 52 cm^{-1} (from 1608 to 1556 cm^{-1}). Significant increases are also obtained for the frequencies of the in plane distortion involving the C5C6 bond ($3a_2$ mode, $+59$ cm^{-1}), of the CS stretches ($3b_2$ mode, $+47$ cm^{-1}), and of the out of plane bending of terminal hydrogen atoms ($4b_1$ mode, $+51$ cm^{-1}). These last three variations indicate that there is a significant increase of the rigidity of the thiole rings in going from TTF to TTF$^+$. All the other modes are essentially unaffected by the ionization process.

Similar trends are found for the TTP/TTP$^+$ pair. Here the largest variation (-169 cm^{-1}) is associated with the C5C6 stretching frequency ($2a_2$ mode), while smaller changes are found for the frequencies of other CC stretches (-44 and -52 cm^{-1} for the $3a_2$ and $2b_2$ modes, respectively). In analogy with the behavior of TTF, we observe decrease both of the frequency of the in plane distortion involving the C5C6 bond ($3a_2$ mode) and of that corresponding to the out of plane of the terminal hydrogen atoms ($4b_1$ mode). At the same time, all the CS stretching modes become softer.

The differences between the neutral TTP molecule and its radical cation are well evidenced in the simulated IR spectra of Figure 4, which have been obtained by associating one Lorentzian function to each computed frequency.

The vibrations involving the CC and CH atom pairs (modes $2a_2$, $3a_2$, and $4b_1$) are well evidenced in the figure since they have a significant intensity, whereas the low-intensity vibrations associated with the CS bonds are not visible on the scale of the plot.

In summary, the presence of the soft inversion motion and the overall geometrical features suggest that the TTP/TTP$^+$ pair has properties similar to those of the TTF/TTF$^+$ pair.

Finally, the electronic structures of TTF and TTP have been investigated using the natural resonance theory (NRT),[53] which provides a molecular electron density analysis in term of classical resonance theory concepts.[54] This analysis has been successfully applied to the study of different organic and inorganic molecules, including radicals (see for instance refs 55 and 56). These computations have required the writing of a proper interface between the Gaussian98 package and the last public release (4.0) of the NBO program, which contains the NRT option.[55]

In Figure 5 are reported the main resonance structures of TTF and TTP, together with the corresponding weights.

As may be seen from this figure both molecules can be described in terms of the same resonance structures, but their relative weights are different. So in TTF the covalent structure

TABLE 2: Harmonic Wavenumbers (cm^{-1}), Intensities (km/mol), and Approximate Assignment for TTF, TTP, and Their Radical Cations[a]

	TTF						
symmetry[b]	B1LYP	expt[c]	TTF^+	assgnmt	TTP	TTP^+	assgnmt
a_1	3229	3083	3233	CH str	3240	3247	CH str
	1624	1555	1536	CCstr	1642	1596	CCstr
	1581	1518	1437	CCstr	1588	1419	CCstr
	1120	1094	1128	CH bend	1101	1111	CH bend
	729	735	747	CS str	627	609	CH bend
	640	639	694	CH bend	471	479	CS str
	472	474	506	CS str	423	429	ring def
	265	247	324	ring def	402	422	ring def
	235	244	264	ring def	202	213	ring def
	37	110	51	ring tors	44	62	ring tors
a_2	3209	3072	3216	CH str	3156	3156	CH str
	1285	1258	1296	CH bend	1417	1411	CH bend
	973	994	1032	CC bend	946	999	CC bend
	864		885	CH bend	829	913	CH bend
	800	800	830	CS str + CH bend	751	773	CS str + CH bend
	615	612	631	CS str + ring def	559	553	CS str + ring def
	413		420	ring def	436	425	ring def
	307	308	302	CC bend	324	348	CC bend
	83		145	CC twist	123	109	CC twist
b_1	3209	3073	3216	CH str	3153	3156	CH str
	1283	1254	1291	CH bend	1416	1408	CH bend
	864	863	884	CS str	1038	1088	CC bend
	830		881	CH bend	829	913	CH bend
	793	794	829	CS str + CH bend	812	938	CS str
	624	639	640	CS str + ring def	729	756	CS str + CH bend
	416	414	431	ring def	570	575	ring def
	109	110	117	CC bend	364	372	CC bend
b_2	3229	3108	3233	CH str	3240	32470	CH str
	1608	1530	1556	CC str	1631	1579	CC str
	1121	1090	1128	CH bend	1111	1120	CH bend
	772	781	819	CS str	631	634	CS str
	726	734	736	CS str	499	442	CS str
	641		695	CH bend	463	505	CH bend
	502		507	CC bend	314	301	CC bend
	430	427	470	ring def	152	235	ring def
	79		86	ring tor	47	63	ring tor

[a] All of the values have been computed at the B1LYP/6-311G(d,p) level. [b] C_{2v} symmetry. [c] From ref 48.

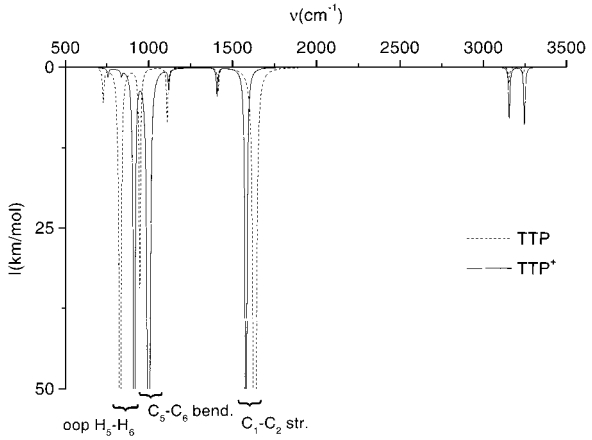

Figure 4. Theoretical IR spectra for tetrathiapentalene and its radical cation. The spectra are reproduced by associating a single Lorentzian function to each computed wavenumber, with a half-height width of 10 cm^{-1}.

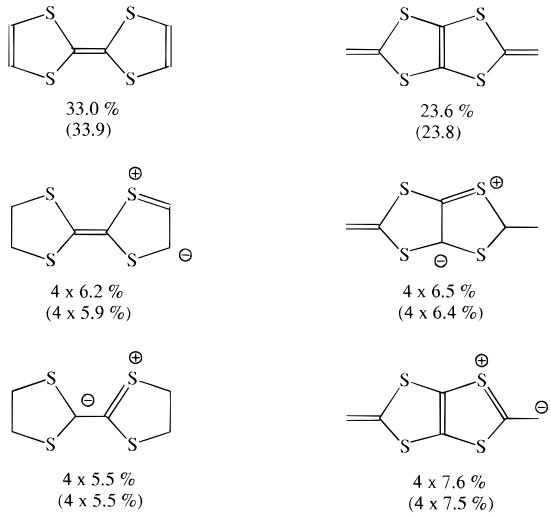

Figure 5. Resonance structures of TTF and TTP obtained from the natural resonance theory both in vacuo and in aqueous solution (in parentheses).

prevails (30%), followed by the structure involving a negative charge of the outermost carbons and a positive charge on the sulfur atoms. Since in these last cases there are four equivalent possibilities, the total weight is 24.8% (4 × 6.2%). The last resonance structure shows a negative charge on the internal carbon atoms, and its weight is 22.0% (4 × 5.5%). In contrast, for TTP the weights of the resonance structures involving charge separation are higher than that assigned to the neutral covalent structure. In fact, the structure with the negative charge on the outermost carbons (C6) contributes 30.4%, while the weight of the other ionic structure is 26%. Finally, the covalent structure is the less favorable (23.6%).

Assuming that the ionization process does not alter the orbital scheme, these conclusions remain valid for the corresponding

TABLE 3: Isotropic Hyperfine Coupling Constants (*a*, G) and Mulliken Atomic Spin Populations (*ρ*) Obtained for the TTF and TTP Radical Cations at the B1LYP Level[a]

	TTF^+			TTP^+	
	ρ	*a*	*a*(expt)	*ρ*	*a*
C_1	0.110 (0.127)	2.19	2.85 ± 0.05[b]	0.190 (0.136)	6.02
C_2	0.110 (0.127)	2.19	2.85 ± 0.05[b]	−0.078 (0.0)	−6.56
S_3	0.170 (0.148)	2.03	4.25 ± 0.05[b] 4.39 ± 0.03[c]	0.134 (0.124)	1.59
C_5	0.027 (0.037)	0.15		0.118 (0.125)	3.02
C_6	0.027 (0.037)	0.15		0.118 (0.125)	3.02
H_6	−0.002 (0.0)	−1.32	1.25 ± 0.02[b] 1.262 ± 0.023[c] 1.26 ± 0.02[d]	−0.008 (0.0)	−5.13

[a] All of the values have been computed at the B1LYP level, using the EPR-II basis set and the B1LYP/6-311G(d,p) geometries, in parentheses are reported the ROB1LYP/EPR-II results. The absolute values of experimental isotropic hyperfine coupling constants are also reported. [b] Reference 6. [c] Reference 7. [d] Reference 5.

cation radicals, thus indicating a tendency to localize the unpaired electron on the external side of the molecule.

In Figure 5 are shown also the weights of the different resonance structures in aqueous solution as obtained from PCM computations. Once again only marginal variations have been found, so that the above trends apply as well as in aqueous solution.

3.2. Spin Distribution and Magnetic Properties. Table 3 collects the hcc's for the $^2B_1$ electronic states of the TTF^+ and TTP^+ radicals. Also in this case solvent effects have been taken into account by PCM computations, but the results are not reported in the table since they are very close to their in vacuo counterparts.

Even if the interpretation of the expectation value for S^2, $\langle S^2 \rangle$, is not straightforward in the framework of DF methods,[57] its value still indicates, at least roughly, the extent of contamination by higher spin states. So the computed B1LYP/EPR-II values, $\langle S^2 \rangle = 0.759$ and 0.764 for TTF^+ and TTP^+, respectively, suggest that we are dealing with essentially pure doublet states, pointing out the reliability of the computed spin properties.

The EPR spectrum of the TTF^+ radical has been studied in detail and three different data sets are available for hydrogen hcc's.[5−8] These values are well reproduced by our computations: in particular, the computed value for H atoms (−1.32 G) is very close to experiments (1.25 ÷ 1.26 G),[5−8] while a slight difference is found for the hyperfine constants of the central C2 and C3 atoms, the B1LYP value (2.2 G) being smaller than the experimental finding (2.9 G).[6] The situation is less favorable for the hcc's of the sulfur atoms, for which the experimental data range between 4.3 and 4.4 G.[6,7] Here, the B1LYP value is 2.03 G, but this difference is probably due to the well-known difficulties of DF methods, including B1LYP, in handling the hyperfine constants of third-row elements in *π*-radicals.[16,58] As a matter of fact the overall hcc's on non-hydrogen atoms of *π*-radicals results from a delicate balance between large and opposite spin polarizations of successive *s* shells. Since these orbitals are characterized by very different shapes of the electron densities, a balanced density functional description of electron exchange is quite difficult. Current pure functionals are generally not very accurate, whereas hybrid models containing a fixed amount of Hartree−Fock exchange lead to a more balanced description of 1s and 2s shells. Inclusion of a third shell perturbs this equilibrium, and the only issue would be to use a different weight of HF exchange for core electrons. Although work is in progress in this connection, the results obtained by the B1LYP functional are at least qualitatively reasonable.

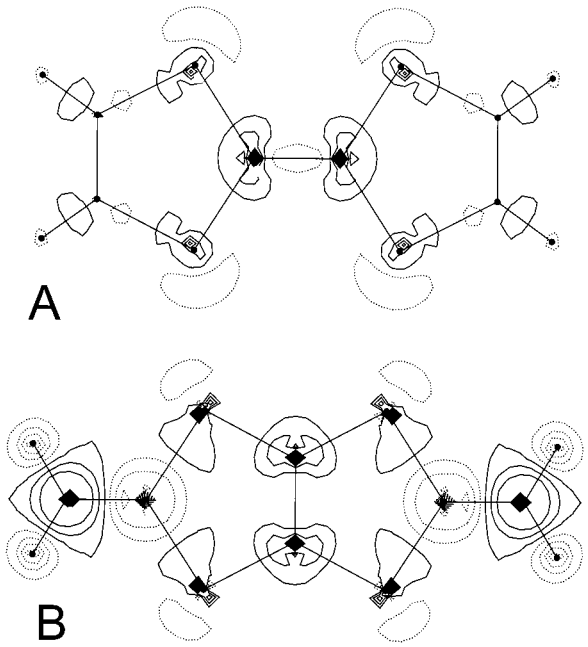

Figure 6. Iso-spin density plots for TTF^+ (A) and TTP^+ (B) radical cations. Contour levels are spaced by 0.005 au starting from the absolute minimum on the C_5 atom.

All the hcc's of non-hydrogen atoms in TTF^+ are positive, whereas negative values are obtained for the C2 atoms of TTP^+. This trend can be better understood by looking at the spin densities of the two radicals shown in Figure 6.

In general terms, the spin densities can be decomposed into three contributions: a delocalization or direct term, which is always positive (or null), a spin polarization or indirect term,[59,60] and a correlation term (neglected in the following qualitative analysis). The spin polarization term takes into account the fact that the unpaired electron interacts differently with the two electrons of a spin-paired bond, since the exchange interaction (which reduces the Coulomb repulsion) is operative only for electrons with parallel spins.[61] This induces a shorter average distance between parallel electrons than between antiparallel ones, leading to the spin polarization pattern characterized by an alternation of positive and negative spin density.[26] The molecular plane of *π* radicals is the nodal plane of the singly occupied molecular orbital (SOMO) and the only contribution to spin densities at nuclei comes from the indirect (spin polarization) contribution.

The spin density map of the TTF^+ radical (Figure 6A) shows only positive contributions on the C and S atoms, while small negative densities are present on hydrogen atoms, due to the spin polarization contribution. A substantial portion of the unpaired spin density resides on the sulfur atoms, in agreement with the experimental interpretation of EPR spectra.[7]

The TTP^+ radical has a completely different spin density plot (Figure 6B), showing an odd-alternate pattern of density, with a significant negative density on the C2 atom. As mentioned above, the delocalization contribution is related to the shape of the SOMO's shown in Figure 7.

The orbital of TTF^+ is delocalized over the whole molecule, showing that all the contributions to the spin density arise from the delocalization term. In contrast the SOMO of TTP^+ has significant contributions from the terminal carbon (C1) and from sulfur atoms (S3 and S4), whereas orbitals belonging to C2 do not participate. The resulting effect is a large *π*-spin population

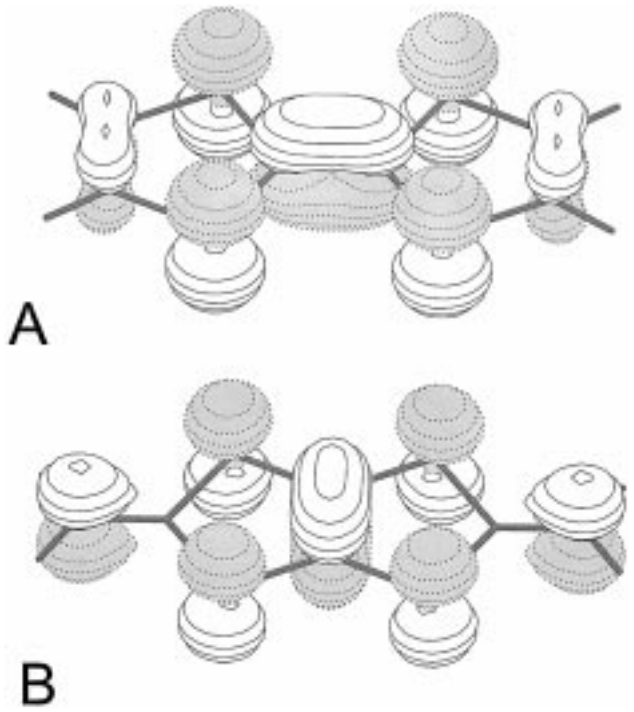

Figure 7. Schematic drawing of the SOMO's of TTF^+ (A) and TTP^+ (B) radicals.

on C1 and S2, which induces, by a spin polarization mechanism, positive spin densities at the corresponding nuclei and negative hcc's at C2 and hydrogens.

We now examine the Mulliken spin population computed from the unrestricted wave function. As expected, the results given in Table 3 reveal a negative spin population at the C2 atom of TTP^+. This results from the fact that spin polarization is directly taken into account in the computation, together with delocalization.This negative contribution totally disappears, of course, at the ROB1LYP level. In contrast no significant variations in spin populations are observed in going from ROB1LYP to UB1LYP computations for TTF^+, thus underlining, once again, the dominant role of the SOMO in determining the spin distribution in this radical.

The spin distribution gives also some indications about the reactivity of the two radicals, since they can be taken as a measure of the radical dimerization. So, TTF is less prone to undergoing dimerization reactions since most of the spin density is localized "inside" the molecule. As a consequence, the TTF^+ radical is stable for a long time in different environments and normal conditions.[5] In contrast the high spin density present on the terminal carbon atoms of the TTP^+ radical is responsible for the high reactivity of this radical.[13]

To complete the comparison between TTF and TTP, adiabatic ionization potentials (IPs) have been computed as the energy differences between neutral and cationic systems at their respective optimized geometries. There is a remarkable agreement between the computed (6.29 eV) and experimental (6.31 eV [57]) values for TTF. A slightly larger value is computed for TTP (6.79 eV), thus suggesting a lower tendency to form CT pairs for TTP with respect to TTF.

4. Conclusions

In the present paper the molecular properties of tetrathiapentalene have been analyzed with the aim of understanding if this molecule has the characteristics to be considered as a new molecular brick in the field of organic conductors. To this end extensive comparison has been done with the analogous tetrathiafulvalene. The results show that the overall structural, electronic, and magnetic properties of TTP and TTP^+ mime those of TTF and TTF^+, especially concerning the floppy inversion motion which is characteristic of organic conducting materials. However, the quite different spin distribution of TTF^+ and TTP^+ radicals has a profound influence on their stability. In particular, the significant spin localization on terminal carbon atoms of TTP^+ can explain its higher reactivity.

From a more general point of view, our study shows that hybrid HF/KS methods provide powerful additional tools for aiding the analysis of structural and magnetic properties, especially when experimental data are limited or concurrent interpretations are possible.

References and Notes

(1) *Magnetism: A Supramolecular Function*; Kahn, O., Ed.; NATO ASI Series C484; Kluwer Academic Publisher: Amsterdam, 1996.

(2) *Molecular Magnetism. From Molecular Assemblies to the Devices*; Coronado, E., Delhaes, P., Gatteschi, D., Miller, J. S., Eds.; NATO ASI Series E 321; Kluwer Academic Publisher: Amsterdam, 1996.

(3) Day, P.; Kurmoo, M.; Mallah, T.; Marsden, I.; Friend, R. H.; Pratt, F. L.; Hayes, W.; Chasseau, D.; Gaultier, J.; Bravic, G.; Ducasse, L. *J. Am. Chem. Soc.* **1992**, *114*, 10722.

(4) Coronado, E.; Galan-Mascaros, J. R.; Gimenez-Saiz, C.; Gomez-Garcia, C. J.; Triki, S. *J. Am. Chem. Soc.* **1998**, *120*, 4671.

(5) Wudl, F.; Smith, G. M.; Hufnagel, E. J. *Chem. Commun.* **1970**, 1453.

(6) Cavara, L.; Gerson, F.; Cowan, D. O.; Lerstrup, K. *Helv. Chim. Acta* **1986**, *69*, 141.

(7) Hibbert, D. B.; Hamedelniel, A. E.; Sutcliffe, L. H. *Magn. Res. Chem.* **1987**, *25*, 648.

(8) Bryce, M. R.; Moore, A. J.; Tanner, B. K.; Whitehead, R.; Clegg, W.; Gerson, F.; Lamprecht, A.; Pfenninger, S. *Chem. Mater.* **1996**, *8*, 1182.

(9) Coffen, D. L.; Chambers, J. Q.; Williams, D. R.; Garrett, P. E.; Canfield, N. D. *J. Am. Chem. Soc.* **1971**, *93*, 2258.

(10) Williams, J. M.; Ferraro, J. R.; Thorn, R. J.; Carlson, K. D.; Geiser, U.; Wang, H. H.; Kini, A. M.; Whangbo, M. H. *Organic Superconductors (Including Fullerenes)*; Prentice Hall: Englewood Cliffs, NJ, 1992.

(11) Demiralp, E.; Dasgupta, S.; Goddard, W. A., III *J. Am. Chem. Soc.* **1995**, *117*, 8154.

(12) Misaki, Y.; Yamabe, T.; Higuchi, N.; Fujiwara, H.; Mori, T.; Tanaka, S. *Angew. Chem., Int. Ed. Engl.* **1995**, *34*, 1222.

(13) Müller, H.; Sahli, F.; Divisia-Blohorn, B. *Tetrahedron Lett.* **1997**, *38*, 3215

(14) Barone, V.; Bencini, A.; di Matteo, A. *J. Am. Chem. Soc.* **1997**, *119*, 10831.

(15) Barone, V.; Adamo, C.; Russo, N. *Chem. Phys. Lett.* **1993**, *212*, 5.

(16) Barone, V. In *Recent Advances in Density Functional Methods*, Part 1; Chong, D. P., Ed.; World Scientific Publishing Co.; Singapore, 1995; p 287.

(17) Barone, V. *Chem. Phys. Lett.* **1996**, *262*, 201.

(18) Adamo, C.; Barone, V.; Fortunelli, A. *J. Chem. Phys.* **1995**, *102*, 384.

(19) Boesch, S. E.; Wheeler, R. A. *J. Phys. Chem. A* **1997**, *101*, 5799.

(20) Noodleman, L.; Peng, C. Y.; Case, D. A.; Mouesca, J. M. *Coord. Chem. Rev.* **1995**, *144*, 199.

(21) Bencini, A.; Totti, F.; Daul, C. A.; Doclo, K.; Fantucci, P.; Barone, V. *Inorg. Chem.* **1997**, *36*, 5022.

(22) Erickson, L. A.; Malkin, V. G.; Malkina, O. L.; Salahub, D. R. *J. Chem. Phys.* **1993**, *217*, 24.

(23) O'Malley, P. J. *J. Phys. Chem.* A **1998**, *102*, 248.

(24) Himo, F.; Graslund, A.; Eriksson, L. A. *Biophys. J.* **1997**, *72*, 1556.

(25) Jolibois, F.; Cadet, J.; Grand, A.; Subra, R.; Rega, N.; Barone, V. *J. Am. Chem. Soc.* **1998**, *120*, 1864.

(26) Adamo, C.; Subra, R.; di Matteo, A.; Barone, V. *J. Chem. Phys.* **1998**, *109*, 10224.

(27) Adamo, C.; Barone, V. *Chem. Phys. Lett.* **1997**, *274*, 242.

(28) Adamo, C.; Barone, V. *J. Chem. Phys.* **1998**, *108*, 664.

(29) Adamo, C.; Barone, V.; Bencini, A.; Totti, F.; Ciofini, I. *Inorg. Chem.* **1999**, *38*, 1996.

(30) Novoa, I. J.; Whangbo, M.; Williams, J. M. *Mol. Cryst. Liq. Cryst.* **1990**, *181*, 25.

(31) Demiralp, E.; Goddard, W. A., III *Synth. Met.* **1995**, *72*, 297.

(32) Demiralp, E.; Goddard, W. A., III *J. Phys. Chem. A* **1997**, *101*, 8128.

(33) Liu, R.; Zhou, X.; Kasmai, H. *Spectrosc. Chim. Acta A* **1997**, *53*, 1241.

(34) Frisch, M. J.; Trucks, G. W.; Schlegel, H. B.; Scuseria, G. E.; Robb, M. A.; Cheeseman, J. R.; Zakrzewski, V. G.; Montgomery, J. A., Jr.; Stratmann, R. E.; Burant, J. C.; Dapprich, S.; Millam, J. M.; Daniels, A. D.; Kudin, K. N.; Strain, M. C.; Farkas, O.; Tomasi, J.; Barone, V.; Cossi, M.; Cammi, R.; Mennucci, B.; Pomelli, C.; Adamo, C.; Clifford, S.; Ochterski, J.; Petersson, G. A.; Ayala, P. Y.; Cui, Q.; Morokuma, K.; Malick, D. K.; Rabuck, A. D.; Raghavachari, K.; Foresman, J. B.; Cioslowski, J.; Ortiz, J. V.; Stefanov, B. B.; Liu, G.; Liashenko, A.; Piskorz, P.; Komaromi, I.; Gomperts, R.; Martin, R. L.; Fox, D. J.; Keith, T.; Al-Laham, M. A.; Peng, C. Y.; Nanayakkara, A.; Gonzalez, C.; Challacombe, M.; Gill, P. M. W.; Johnson, B.; Chen, W.; Wong, M. W.; Andres, J. L.; Gonzalez, C.; Head-Gordon, M.; Replogle, E. S.; Pople, J. A. G*aussian 98* (Revision A.6); Gaussian Inc.: Pittsburgh, PA, 1998.

(35) Frisch, *Æ.*; Frisch, M. J. *Gaussian 98 User's Reference*; Gaussian, Inc.: Pittsburgh, PA, 1998.

(36) Becke, A. D. *Phys. Rev. B* **1988**, *38*, 3098.

(37) Lee, C.; Yang, W.; Parr, R. G. *Phys. Rev. B* **1988**, *37*, 785.

(38) Krishnan, R.; Binkley, J. S.; Seeger, R.; Pople, J. A. *J. Chem. Phys.* **1980**, *72*, 650.

(39) Curtiss, L. A.; Raghavachari, K.; Redfern, P. C.; Pople, J. A. *Chem. Phys. Lett.* **1997**, *270*, 419.

(40) Barone, V.; Adamo, C. *J. Chem. Phys.* **1996**, *105*, 11007.

(41) Rega, N.; Cossi, M.; Barone, V. *J. Chem. Phys.* **1996**, *105*, 11060.

(42) Weltner, W., Jr. *Magnetic Atoms and Molecules*; Dover: New York, 1989.

(43) *Molden*, Release 3.4; CAOS/CAMM Center: The Netherlands, 1998.

(44) Cooper, W. F.; Kenny, N. C.; Edmonds, J. W.; Nagel, A.; Wudl, F.; Coppens, P. *Chem. Commun.* **1971**, 889.

(45) Hargittai, I.; Brunvoll, J.; Kolonits, M.; Khodorkovsky, V. *J. Mol. Struct.* **1994**, *317*, 273.

(46) Kobayashi, H.; Kobayashi, A.; Yukiyoshi, S.; Saito, G.; Inkuchi, H. *Bull. Chem. Soc. Jpn.* **1986**, *59*, 301.

(47) Berlinsky, A. J.; Hoyano, Y.; Weiler, L. *Chem. Phys. Lett.* **1977**, *45*, 419.

(48) Bozio, R.; Zanon, R.; Girlando, A.; Pecile, C. *J. Chem. Phys.* **1979**, *71*, 2282.

(49) Minichino, C.; Barone, V. *J. Chem. Phys.* **1994**, *100*, 3717.

(50) Barone, V.; Minichino, C. *THEOCHEM* **1995**, *330*, 325.

(51) Cossi, M.; Barone, V.; Cammi, R.; Tomasi, J. *Chem. Phys. Lett.* **1996**, *255*, 327.

(52) Cossi, M.; Barone, V. *J. Chem. Phys.* **1998**, *109*, 6246.

(53) Glendening, E. D.; Badenhoop, J. K.; Weinhold, F. University of Wisconsin Technical Report WIS-TCI-803; University of Wisconsin: Madison, 1994.

(54) Reed, A. E.; Curtiss, L. A.; Weinhold, F. *Chem. Rev.* **1988**, *88*, 899.

(55) *NBO 4.0 program.*, Glendening, E. D., Badenhoop, J. K., Reed, A. E., Carpenter, J. E., Weinhold, F., Eds.; Theoretical Chemistry Institute, University of Wisconsin: Madison, 1996.

(56) Eiden, G.; Weinhold, F.; Weisshaar, J. C. *J. Chem. Phys.* **1991**, *95*, 8665.

(57) Wang, J.; Becke, A. D.; Smith, V. H., Jr. *J. Chem. Soc.* **1995**, *102*, 3477.

(58) Barone, V. Unpublished results.

(59) McConnell, H. M. *J. Chem. Phys.* **1956**, *24*, 633.

(60) Ellinger, Y.; Rassat, A.; Subra, R.; Berthier, G. *J. Am. Chem. Soc.* **1973**, *95*, 2372. Ellinger, Y.; Subra, R.; Levy, B.; Millie, P.; Berthier, G. *J. Chem. Phys.* **1975**, *62*, 10.

(61) Claxton, T. A. *Chem. Soc. Rev.* **1995**, 437.

(62) Lichtenberger, D. L.; Johnston, R. L.; Hinkelmann, K.; Suzuki, T.; Wudl, F. *J. Am. Chem. Soc.* **1990**, *112*, 3302.